

Identification of Individual Si-Rich Particles Derived from Kosa Aerosol by the Alkali Elemental Composition

Tomohiro Kyotani*[#] and Satoshi Koshimizu

Earth Science Division, Yamanashi Institute of Environmental Sciences, Kenmarubi, Kamiyoshida, Fujiyoshida, Yamanashi 403-0005

(Received October 16, 2000)

A method of scanning electron microscopy-energy dispersive X-ray microanalysis (SEM-EDX) has been investigated for the identification of individual Si-rich particles derived from Kosa aerosol. The elemental composition of individual Si-rich particles (α -quartz) having SiO_2 content over 80% was determined by SEM-EDX using a standardless $\phi(\rho z)$ correction program, and the results were normalized to 100% on the basis of oxide composition. The distribution of $(\text{Na}_2\text{O} + \text{K}_2\text{O})/\text{SiO}_2(\%)$ in individual Si-rich particles from real airborne particulate matters showed a sharp and clear seasonal variation. It was found that the distribution was closer to those in the China loess and desert sand in spring time compared to those of the non-Kosa aerosol, the distribution could be successfully used as an effective indicator. The distribution of $(\text{MgO} + \text{CaO})/\text{SiO}_2(\%)$ was also used for discrimination from Si-rich particles in some Japanese volcanic rocks such as Andesites. Individual Si-rich particles derived from Kosa aerosol were clearly discriminated from those derived from the Japanese igneous rocks by the proposed method. These results suggest that the alkali elemental composition of individual Si-rich particles is a useful indicator to identify the Kosa particles and to investigate transportation of the Kosa aerosol.

Asian dust-storm particles, called as the Kosa aerosol in Japan, originate from arid and semi-arid areas of China,¹ mainly during the spring time, and spread to vast areas of northern China being driven by the wind torrents from the northwest or west. It has been shown that the Kosa aerosol traverses the China continent, crosses Yellow sea and Korea peninsula, and reaches Japan^{2–6} and even as far as the north Pacific Ocean.^{2,6–12} The chemical compositions and the discriminating methods of Kosa aerosol have been studied by many investigators using bulk analysis, but the information obtained is only for average compositions,^{2–11,13–17} and the contribution to the atmospheric environment has been confirmed usually by the increase of total concentrations of characteristic components or elements of the China loess and desert sand in suspended particulate matter (SPM). In these methods, strict evaluation not only of the contribution of Kosa aerosol but also of the origins of individual particles, is not easy for SPM, which consists of complicated multi-component mixtures.¹⁸ Furthermore, the discrimination of individual particles derived from China loess or desert sand and Japanese rocks or soils, so far has been impossible.

Although the elemental compositions of individual Kosa particles have been investigated by electron probe microanalysis,^{12,19} most researches have been carried out concentrating on the chemical reactions and formation of secondary particulates on the particles or the internal mixture of minerals and sea-salt without information on the mineral compositions, because the particles collected were directly analyzed without surface washing. Thus, the pieces of information obtained were only

average compositions of aggregates. Therefore, the elemental composition of individual particles in SPM has not yet been used as an indicator for the identification of Kosa particles.

The aim of this paper is to establish the method for identification of individual Kosa particles in airborne particulate matter by the alkali elemental composition. Si-rich particles having SiO_2 content over 80% such as α -quartz were examined as an effective indicator of Kosa particles and the elemental composition of individual Si-rich particles was determined by scanning electron microscopy-energy dispersive X-ray microanalysis (SEM-EDX). Individual Si-rich particles derived from Kosa aerosol in real airborne particulate matter were clearly identified by differences of the distribution areas of $(\text{Na}_2\text{O} + \text{K}_2\text{O})/\text{SiO}_2(\%)$.

Experimental

Airborne Particulate and Rain Water Samples. SPM samples were collected on the mixed cellulose ester membrane filters (Advantec, A300A110C, 3.0 μm in pore size, 110 mm in diameter) for 13 days by a low-volume air sampler with a cyclone classifier ($< 10.0 \mu\text{m}$) (Shintaku Machine Manuf., Model S-2) with a flow rate of 20 L min^{-1} at Kofu and Fujiyoshida, Yamanashi Pref., central Japan in 1995. Other SPM samples were collected on the polycarbonate filters (Millipore, ATTP, 0.8 μm in pore size, 47 mm in diameter) for 3–5 days by the same sampler with a flow rate of 20 L min^{-1} at Fujiyoshida, Yamanashi Pref., central Japan, in 2000. PM10 samples were collected on the regenerated cellulose filters (Fuji Photo Film, FR-100, 1.0 μm in pore size, 47 mm in diameter) for 7–12 days by a low-volume air sampler (Rupprecht & Patashnick Co., Partisol Model 2000) with a flow rate of 16.7 L min^{-1} at Kofu in 1996–1997.

Rain water samples were collected by sequential collection ev-

[#] Domestic Research Fellow, Japan Science and Technology Corporation, Honmachi, Kawaguchi, Saitama 332-0012

ery 1 mm (5 mL) of precipitation from the beginning of rainfall using Horiba Raingoround II metal-free rain-water sampler. The particles in rain waters were filtered off through a 0.45 μm membrane filter, and the initial precipitation (1 mm) was used in this study.

Japanese Igneous Rock, China Loess and Desert Sand Powders. In order to obtain the general elemental composition of Si-rich particles in the Japanese igneous rocks, China loess and desert sand, some igneous rock powders²⁰ e.g., granite (JG-2), granodiorite (JG-1a, JG-3), andesite (JA-1, JA-2), basalt (JB-2) and rhyolite (JR-1) were supplied by the Geological Survey of Japan. The China loess (CJ-1), and simulated Asian mineral dust (CJ-2) prepared from Tengger desert sand were supplied by the National Research Center for Environmental Analysis and Measurement, China. They were used after hydrochloric acid (1+1) treatment for SEM-EDX analysis. In this study, the particles with size below 10 μm were used for analysis.

Sample Preparation. All of the reagents used were of analytical-reagent grade. Deionized and distilled water was used throughout. Hydrophilized poly (tetrafluoroethylene) membrane filters (Millipore, Omunipore JH, 0.45 μm in pore size and 25 mm in diameter) were used for filtering out the residual particles after hydrochloric acid washing. The pieces of 5 mm in diameter cut from the filters were used for particle analysis. Particles on the filters were washed in a 10 mL volume of hydrochloric acid (1+1) for 20 min by ultrasonication. The residual particles were filtered off through a 0.45 μm membrane filter, and washing with water of 3 mL was repeated for 5 times to remove any hydrochloric acid from the particles on the filters. After drying for 30 min at 110 $^{\circ}\text{C}$ in an electric oven, the particles on the filters were detached by both sides-adhesive carbon tape and were fixed on the aluminum sample stands (15 mm in diameter, 5 mm in height) for SEM-EDX. Thereafter, the particles were carbon coated (~ 200 \AA) and the specimens were subjected to the SEM-EDX analysis.

Analytical Method. The particles were examined with a scanning electron microscope (SEM, Hitachi S-3000N) equipped with an energy dispersive X-ray microanalyzer (EDX, Horiba EMAX550). The elemental analysis by EDX was carried out on accelerating voltage = 20 kV, probe current = 0.3 nA and dead time = 20–30%. The takeoff angle for the EDX detector was fixed at 35 $^{\circ}$. These conditions were found to be suitable for good X-ray analysis and allowed reasonable secondary electron imaging. The electron beam was usually irradiated at the central part of an individual particle to get the average composition, and the data was accumulated for 100 s. Particles with radii over 1.0 μm were used for analysis in this study. For the qualitative analysis, an element in the particle was determined when the characteristic X-ray intensity was three times standard deviation (σ) of the background intensity under the peak. For the quantitative analysis, X-ray analysis data were processed by a standardless $\phi(\rho z)$ routine supplied by Horiba, and the results were normalized to 100% on the basis of oxide composition.

Results and Discussion

Analysis of Si-Rich Particles by SEM-EDX. SEM-EDX is an effective method for the elemental analysis of micro atmospheric particles, which have irregular shape or rough surface.^{21–26} Therefore, the elemental composition of individual particles in SPM has been determined by many investigators by using standardless-based EDX.^{12,25,26} However, they have analyzed the particles directly without surface washing, as a

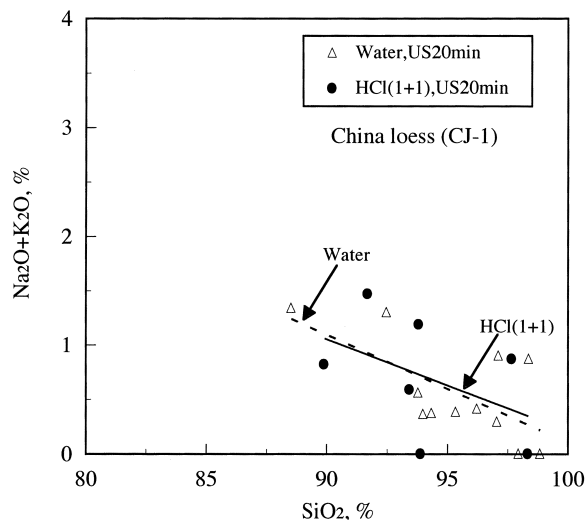


Fig. 1. Effects of water and hydrochloric acid washing on the distribution of $(\text{Na}_2\text{O}+\text{K}_2\text{O})/\text{SiO}_2$ in Si-rich particles from China loess (CJ-1).

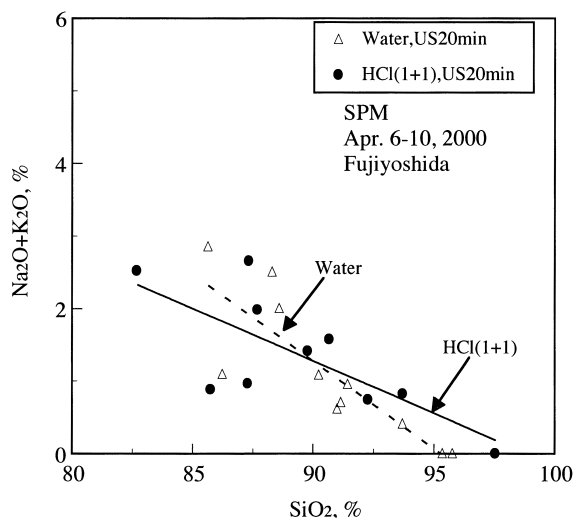


Fig. 2. Effects of water and hydrochloric acid washing on the distribution of $(\text{Na}_2\text{O}+\text{K}_2\text{O})/\text{SiO}_2$ in Si-rich particles from SPM collected at Fujiyoshida in Apr. 6–10, 2000.

result of which only the average compositions of aggregates are available. In the present work, hydrochloric acid washing was carried out prior to SEM-EDX in order to disperse the individual mineral particles and clean the surface. Figures 1 and 2 show the effects of water and hydrochloric acid (1+1) washing procedures on the distributions of $(\text{Na}_2\text{O}+\text{K}_2\text{O})/\text{SiO}_2$ (%) in Si-rich particles from China loess (CJ-1) and SPM collected at Fujiyoshida on Apr. 6–10, 2000, respectively. These results indicated that the dissolution of alkaline elements from Si-rich particles during hydrochloric acid washing can be neglected. Surfaces of most Si-rich particles, such as quartz or volcanic glass, were relatively plate-like and flat compared to those of other particles such as soot, fly ash, iron oxides, sulfates, or carbonates. Therefore, the particles were directly subjected to the SEM-EDX using a standardless $\phi(\rho z)$ correction program

Table 1. Analytical Results of Glass Particles Having Irregular Shape and Rough Surface by SEM-EDX using Standardless $\Phi(\rho z)$

Rhyolite (JR-1) Certified value, % as bulk composition ^{a)}	Na ₂ O	MgO	Al ₂ O ₃	SiO ₂	P ₂ O ₅	K ₂ O	CaO	TiO ₂	MnO	Fe ₂ O ₃
	4.02	0.12	12.83	75.45	0.021	4.41	0.67	0.11	0.099	0.89
1	4.7		13.2	77.3		4.2	0.54			0.65
2	3.9		12.9	78.2		4.5	0.54			0.63
3	5.0		13.6	76.9		4.0	0.74			0.79
4	4.3		13.3	77.5		4.1	0.5			0.80
5	5.6		15.6	74.6		4.2	0.42			0.75
6	3.8		14.9	77.6		3.7	0.64			0.53
7	5.2		13.5	76.6		4.2	0.59			0.71
8	4.7		13.0	77.5		4.4	0.35			0.5
9	4.4		13.8	77.5		4.1	0.50			0.71
10	5.3		14.1	76.6		4.3	0.60			0.57
Av ^{b)}	4.7		13.8	77.0		4.2	0.54			0.66
$\sigma^c)$	0.57		0.82	0.93		0.21	0.10			0.10
RSD, %	12		5.9	1.2		5.0	19			15
Recovery, %	117		108	102		95	81			74

a) Cited from the Ref. 20. b), c) Averages and deviations were calculated from measurements of independent ten particles.

Blank space: Not detected or trace amounts near to their detection limits.

after hydrochloric acid washing. No polishing procedures of particle surface were done, as such polished surfaces do not provide original information on morphological features.

For checking the reliability of the standardless $\Phi(\rho z)$ data, the glass particles (rhyolite, JR-1) were directly analyzed by the method described above without polishing their surfaces. Lengths measured for both short and long axis of particles were 2–9 μm (av 5 μm) and 2–14 μm (av 7 μm), respectively. Five repetitive measurements of the same particle showed reasonable precisions; relative standard deviations (RSDs) were 3.3, 0.3, 0.3, 1.7, 7.1 and 11% for sodium, aluminum, silicon, potassium, calcium and iron, respectively. Ten independent particles were also analyzed in order to evaluate the effects of irregular shape and rough surface. As shown in Table 1, the measurements gave sufficient RSDs and analytical results of the elements detected were in good agreement with the certified values²⁰ as bulk composition without polishing the particle surface, except for calcium and iron, of relatively low contents. The detection limit (DL) was evaluated by the following relation: $\text{DL} = (3C\sigma)/I_{\text{net}}$, where C is the concentration (wt%) of analyte in JR-1, I_{net} is the peak net intensity and σ is the standard deviation of the background intensity under the peak. The DL of elements having sufficient RSDs of measured intensity and contents were as follows; Na₂O:0.30%, Al₂O₃:0.56%, SiO₂:0.39%, K₂O:0.21%, CaO:0.18%, Fe₂O₃:0.10%. The DL of other elements could not be directly determined due to the lack of adequate standard specimens. However, the values were presumed to be near to those of neighboring elements in X-ray spectrum. Although the DL of aluminum was higher compared to those of other elements because of the aluminum $K\alpha$ -line from the sample stand, the value could be neglected compared to those from real Si-rich particles.

In the present work, the particles having SiO₂ content over 80% were referred to as Si-rich particles. Most of the Si-rich particles are presumed to be quartz, because it is the major component in silicate minerals from the China loess and desert

sand.²⁷ Major elements detected by SEM-EDX in the individual Si-rich particles were sodium, magnesium, aluminum, silicon, phosphorus, potassium, calcium, titanium, manganese and iron. Aluminum was detected in all Si-rich particles. When silicon and aluminum were detected with high background, the particle was regarded as a soot.²⁸ Figure 3 shows examples of the number frequency (%) of elements detected in Si-rich particles from SPM, rain water, China loess, desert sand and Japanese igneous rocks. Magnesium, potassium and iron were detected frequently in Si-rich particles from SPM and rain water collected in the spring time. Besides these elements, calcium was detected frequently in rain water, reflecting the different sources of the China loess or desert sand, compared to SPM collected in different periods. Magnesium, potassium and iron were also detected frequently in Si-rich particles from the China loess (CJ-1) and Tengger desert sand (CJ-2). Sodium instead of magnesium, and sodium and calcium together with the above three elements were detected frequently in Si-rich particles from granite (JG-2) or granodiorite (JG-1a) and andesite (JA-1), respectively. Si-rich particles were rarely detected in basalt (JB-2). Therefore, although the discrimination of the Kosa particles seem to be possible by the simultaneous detection of magnesium, potassium and iron, strict evaluation on the basis of these elements was difficult.

Figure 4 shows examples of the distributions of (Na₂O+K₂O)/SiO₂ (%) within the ranges of SiO₂ from 60 to 100% in individual particles from SPM, Tengger desert sand (CJ-2) and basalt (JB-2), and schematic diagram of the composition ranges of main minerals in SPM. Each point indicates an individual particle. In this range of SiO₂ (%), the major mineral components in real airborne particulate matter are presumed to be as follows: α -quartz, volcanic glass, plagioclase, alkali feldspars and clay minerals. However, strict information on the crystal structures of individual mineral particles was not obtained, because the application of X-ray micro-diffractometer to micro particles below 10 μm in diameter was difficult.

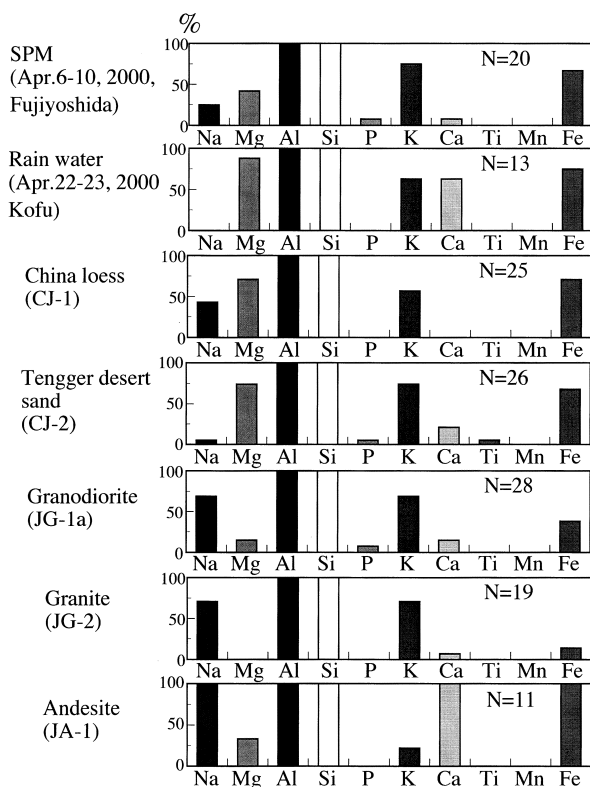


Fig. 3. Number frequency (%) of elements detected in Si-rich particles ($\text{SiO}_2 \geq 80\%$). N indicates the total number of Si-rich particles measured. Number frequencies of elements are the relative ratios of number of particles which contain interest elements to the total number (N) of Si-rich particles measured.

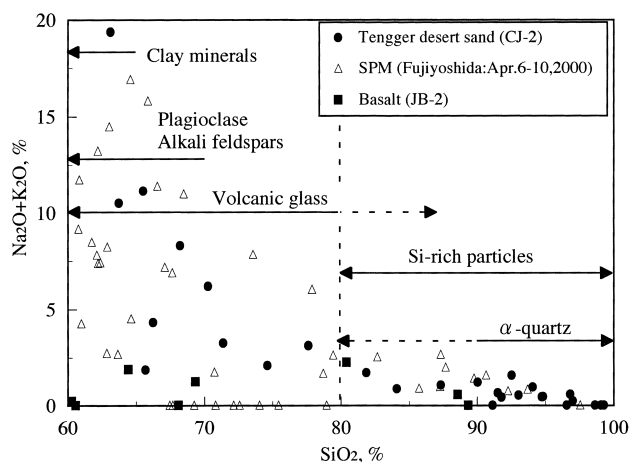


Fig. 4. Examples of the distributions of $(\text{Na}_2\text{O} + \text{K}_2\text{O})/\text{SiO}_2$ in individual particles from SPM, Tengger desert sand and basalt, and schematic diagram of the composition ranges of main minerals in SPM.

In this study, the relationship between the sum of the contents of alkaline elements ($\text{Na}_2\text{O} + \text{K}_2\text{O}$) and the content of SiO_2 in individual Si-rich particles was examined as an indicator.

Discrimination of Si-Rich Particles in China Loess, Desert Sand and Japanese Igneous Rocks. Si-rich parti-

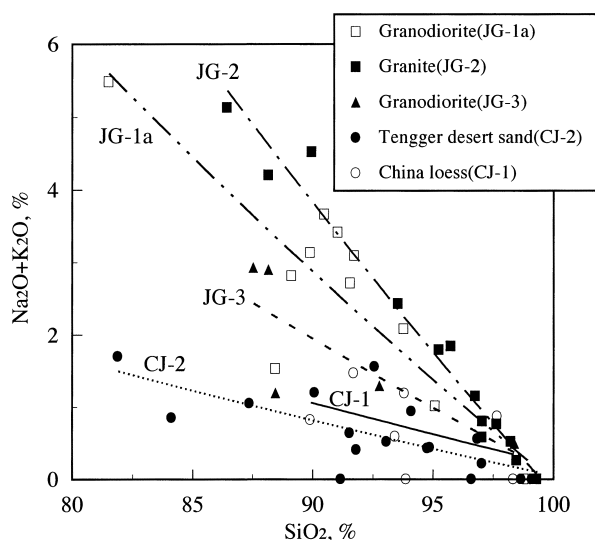


Fig. 5. Distributions of $(\text{Na}_2\text{O} + \text{K}_2\text{O})/\text{SiO}_2$ in Si-rich particles from Japanese plutonic rocks (granite and granodiorites), China loess and desert sand.

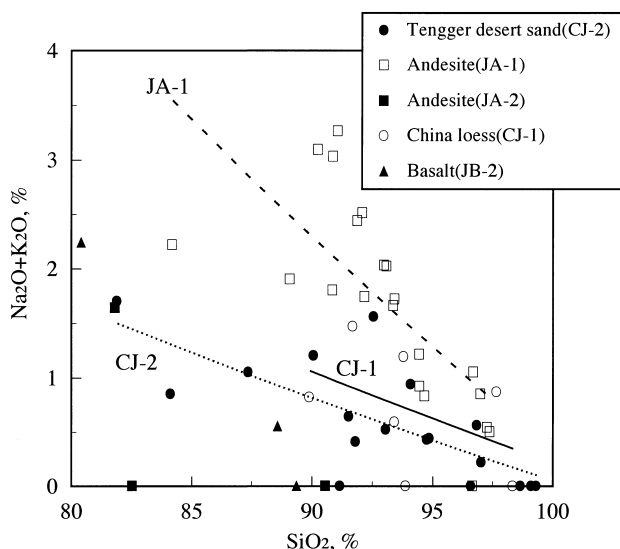


Fig. 6. Distributions of $(\text{Na}_2\text{O} + \text{K}_2\text{O})/\text{SiO}_2$ in Si-rich particles from Japanese volcanic rocks (andesites and basalt), China loess and desert sand.

cles in the real airborne particulate matters consist of particles derived from a variety of sources, e.g., China loess, desert sand and Japanese igneous rocks. Therefore, the discrimination of Si-rich particles in China loess, desert sand and Japanese igneous rocks was examined. Figures 5 and 6 show distributions of $(\text{Na}_2\text{O} + \text{K}_2\text{O})/\text{SiO}_2$ (%) in Si-rich particles from granite (JG-2) and granodiorites (JG-1a and JG-3), and andesites (JA-1 and JA-2) and basalt (JB-2), compared to those from China loess (CJ-1) and Tengger desert sand (CJ-2), respectively. Each point expresses one individual Si-rich particle. Initially, it was expected that the discrimination between Japanese plutonic rocks, e.g., granites or granodiorites, and China loess or desert sand would be the most difficult due to low volcanic activities in the inland areas of China continent. However, the distribu-

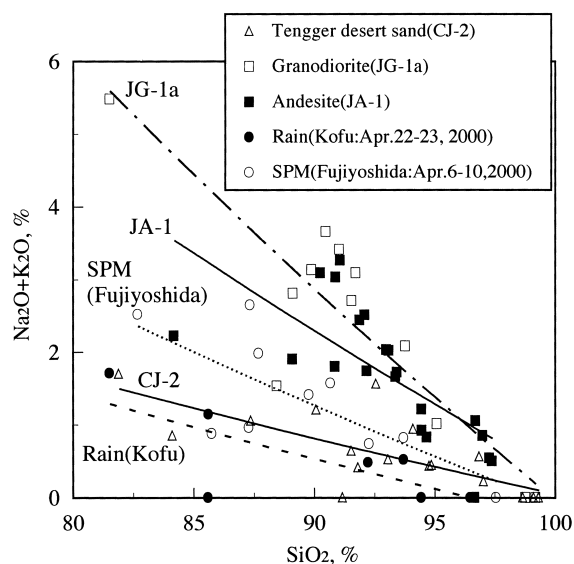


Fig. 7. Distributions of $(\text{Na}_2\text{O} + \text{K}_2\text{O})/\text{SiO}_2$ in Si-rich particles from granodiorite, andesite, Tengger desert sand, SPM and rain water.

tions of $(\text{Na}_2\text{O} + \text{K}_2\text{O})/\text{SiO}_2$ (%) obtained from individual Si-rich particles showed a sharp and clear difference. China loess (CJ-1) and Tengger desert sand (CJ-2) showed similar distributions, and these widely differed from those of the Japanese igneous rocks. Si-rich particles were rarely detected in andesite (JA-2) and basalt (JB-2). Therefore, it was found that the contributions of Si-rich particles from volcanic rocks such as JA-2 and JB-2 can be neglected in case of the Kosa particles identification.

Figure 7 shows a comparison in the distributions of $(\text{Na}_2\text{O} + \text{K}_2\text{O})/\text{SiO}_2$ (%) in Si-rich particles from SPM collected at Fujiyoshida, rain water collected at Kofu, granodiorite (JG-1a), andesite (JA-1) and Tengger desert sand (CJ-2). The distributions of $(\text{Na}_2\text{O} + \text{K}_2\text{O})/\text{SiO}_2$ (%) in Si-rich particles from SPM and rain water collected in spring time showed similar observations to that of the desert sand, although the chemical compositions of those from rain water may be changed from the original compositions, if they were exposed to the clouds with high acidity for a long time. However, the distributions of JA-1 and SPM collected at Fujiyoshida were somewhat similar in low- SiO_2 (%) area. Figure 8 shows the distributions of $(\text{MgO} + \text{CaO})/\text{SiO}_2$ (%) in Si-rich particles from andesite JA-1 and SPM collected at Fujiyoshida. Use of $(\text{Na}_2\text{O} + \text{K}_2\text{O})/\text{SiO}_2$ (%) together with $(\text{MgO} + \text{CaO})/\text{SiO}_2$ (%) was recommended for the discrimination of Si-rich particles in Japanese volcanic rocks such as andesites. These results show that the differences in distribution areas of $(\text{Na}_2\text{O} + \text{K}_2\text{O})/\text{SiO}_2$ (%) are larger compared to the ranges of analytical errors and significance.

Seasonal and Temporal Variations of the Distribution of $(\text{Na}_2\text{O} + \text{K}_2\text{O})/\text{SiO}_2$ (%) in Si-Rich Particles from Real Airborne Particulate Matters. Figure 9 shows the temporal variation of the distribution of $(\text{Na}_2\text{O} + \text{K}_2\text{O})/\text{SiO}_2$ (%) in Si-rich particles from SPM collected at Fujiyoshida in 2000. Except for spring time (March–May), Si-rich particles were rarely detected in SPM from Fujiyoshida. The distributions of $(\text{Na}_2\text{O} + \text{K}_2\text{O})/\text{SiO}_2$ (%) in Si-rich particles detected in spring

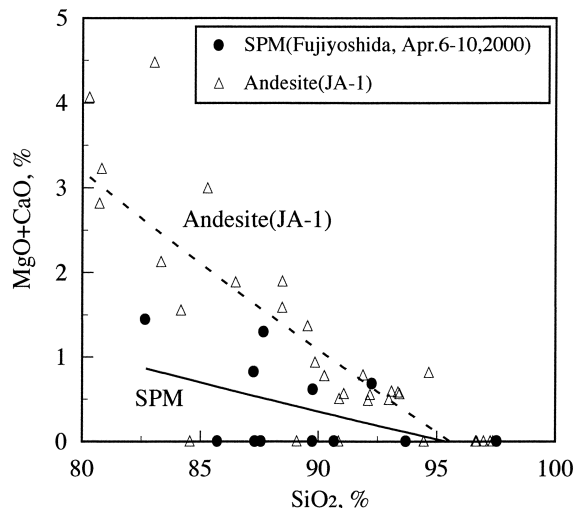


Fig. 8. Distributions of $(\text{MgO} + \text{CaO})/\text{SiO}_2$ in Si-rich particles from andesite and SPM collected at Fujiyoshida.

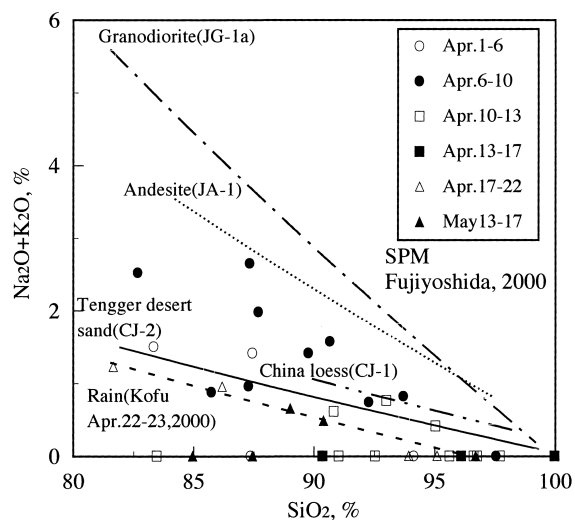


Fig. 9. Temporal variation of the distribution of $(\text{Na}_2\text{O} + \text{K}_2\text{O})/\text{SiO}_2$ in Si-rich particles from SPM collected at Fujiyoshida in 2000.

Lines indicate the distribution areas of granodiorite (JG-1a), andesite (JA-1), China loess (CJ-1), Tengger desert sand (CJ-2) and rain water collected at Kofu in Apr. 22–23, 2000.

time correspond well to those of China loess and desert sand. Airborne particulate matters collected from the locations surrounding Mt. Fuji contain quartz of lower concentration. It has been known that the basaltic geology around Mt. Fuji originated from eruptive materials containing low percentages of quartz. A lower amount of quartz should be found in the geological materials in Fujiyoshida that are mainly basaltic. Therefore, it was suggested that the contributions of Si-rich particles from the locations surrounding Mt. Fuji could be neglected even in spring time where wind erosion of land and rise of the particles from the ground occur easily. As a result, it was presumed that most of the Si-rich particles detected in SPM from Fujiyoshida in spring time were derived from the

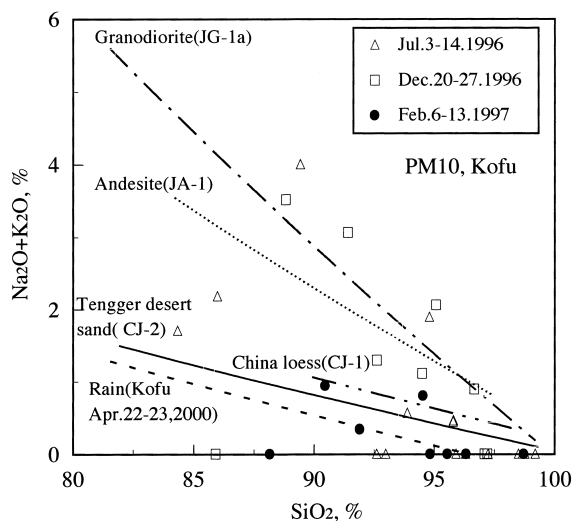


Fig. 10. Seasonal variation of the distribution of $(\text{Na}_2\text{O} + \text{K}_2\text{O})/\text{SiO}_2$ in Si-rich particles from PM10 collected at Kofu in 1996 and 1997.

Lines indicate the distribution areas of granodiorite (JG-1a), andesite (JA-1), China loess (CJ-1), Tengger desert sand (CJ-2) and rain water collected at Kofu in Apr. 22–23, 2000.

Kosa aerosol. Although some particles did not distribute in the areas of China loess and desert sand, they were presumed to arise from Japanese igneous rocks. As a matter of fact, it was found that the Si-rich particles in Kosa aerosol collected during Apr. 6–10, 2000 originated from a different source compared to those collected in other periods even in spring time.

In order to obtain the better information on the distribution of Si-rich particles derived from Japanese igneous rocks, the airborne particles at Kofu that are mainly granitic and sedimentary in nature were analyzed. Figures 10 and 11 show the seasonal variations in the distributions of $(\text{Na}_2\text{O} + \text{K}_2\text{O})/\text{SiO}_2$ (%) in Si-rich particles from PM10 and SPM, respectively, from Kofu City. As clarified from these results, the distribution showed a sharp and clear seasonal variation. In winter (Dec. and Jan.), the distributions of $(\text{Na}_2\text{O} + \text{K}_2\text{O})/\text{SiO}_2$ (%) showed a similar tendency even in the different years, and corresponded well not to those of the China loess and desert sand but to those of granitic rocks. In February, the distribution gradually became closer to those of China loess and desert sand. In summer, when the contribution of Kosa aerosol is presumed to be low or negligible, Si-rich particles detected in SPM are characteristic of locations surrounding Kofu, and the distribution differed widely from that of Kosa aerosol in spring time. However, some particles were distributed in areas of China loess or desert sand. This suggests that the weak Kosa aerosol comes flying as a background except in spring time.²⁹ In the spring time, the distribution of $(\text{Na}_2\text{O} + \text{K}_2\text{O})/\text{SiO}_2$ (%) is very close to those of not only China loess and desert sand but also of Kosa aerosol collected at Fujiyoshida. In Fig. 11, the bulk concentrations ($0.45 \mu\text{g m}^{-3}$) of quartz from SPM collected in Mar. 15–28, increased roughly twice of that ($0.20 \mu\text{g m}^{-3}$) in Mar. 2–15, and the distribution area of $(\text{Na}_2\text{O} + \text{K}_2\text{O})/\text{SiO}_2$ (%) also widely changed.

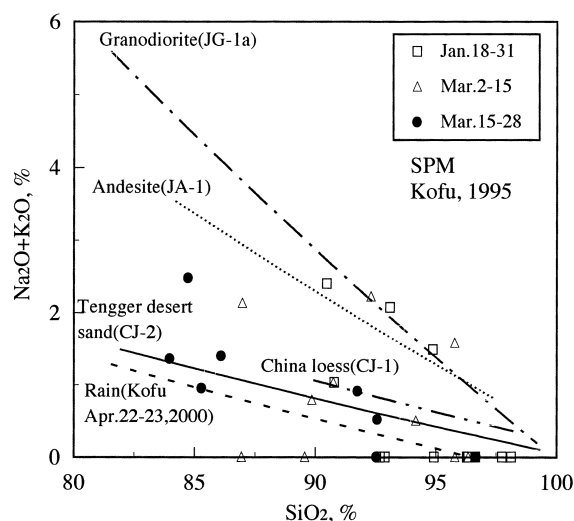


Fig. 11. Temporal variation of the distribution of $(\text{Na}_2\text{O} + \text{K}_2\text{O})/\text{SiO}_2$ in Si-rich particles from SPM collected at Kofu in 1995.

Lines indicate the distribution areas of granodiorite (JG-1a), andesite (JA-1), China loess (CJ-1), Tengger desert sand (CJ-2) and rain water collected at Kofu in Apr. 22–23, 2000.

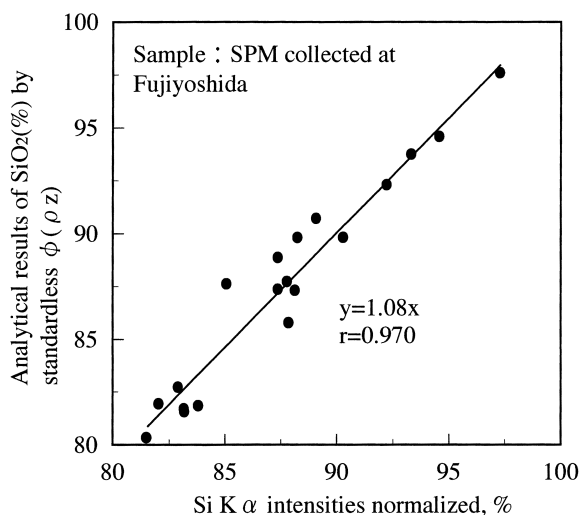


Fig. 12. Relationship between analytical results of SiO_2 (%) by standardless $\phi(\rho z)$ calculation method and Si $K\alpha$ intensities normalized to the total sum of characteristic X-ray intensities of elements with atomic number over 11.

Figure 12 shows the relationship between the contents of SiO_2 (%) determined by standardless $\phi(\rho z)$ and Si $K\alpha$ intensities normalized to the total sum of characteristic X-ray intensities of elements with atomic number over 11. They showed good correlation with each other. Osán et al.²³ described the particles having Si $K\alpha$ normalized intensities over 80% quartz, without X-ray micro-diffraction analysis. According to Osán et al., the particles having SiO_2 content over 80% obtained by standardless $\phi(\rho z)$ can be regarded as quartz. Furthermore, the minimum content of SiO_2 in quartz was confirmed as follows. The atmospheric concentration ratio (2.3) of α -quartz in

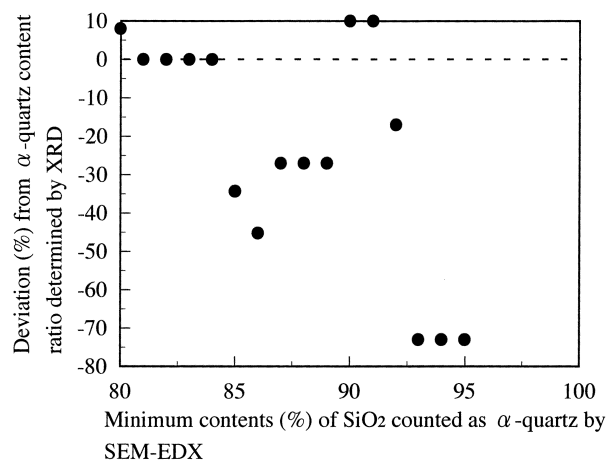


Fig. 13. Comparison among the bulk content ratio of α -quartz determined by XRD and the content ratios of those calculated from the number of Si-rich particles counted by SEM-EDX.

Two SPM samples collected at Kofu in Mar. 15–28 and Mar. 2–15, 1995 were used, and the number of particles counted were 45 and 57, respectively.

SPM collected on Mar. 15–28 to that for Mar. 2–15, 1995, was determined by ordinary X-ray diffraction analysis (XRD) after preconcentration,³⁰ and the α -quartz content ratios (A) among two samples by SEM-EDX were calculated from the numbers of Si-rich particles counted by changing the definition of minimum content of SiO₂ as α -quartz. Deviation from the ratio determined by XRD was evaluated by A/2.3. The results are shown in Figure 13. When the minimum content of SiO₂ counted as α -quartz by SEM-EDX were 80–85%, they correlated well. As a result, although there may be volcanic glass in low SiO₂ area (80–85%), the particles having SiO₂ content over 80% could be regarded as α -quartz.

These results suggest that the individual α -quartz particles in airborne particulate matters are a useful indicator to identify the Kosa particles and to investigate the transportation of Kosa aerosol. The present method can not only identify the Kosa particles, but also can provide direct information on the sources of other Si-rich particles.

The authors thank Dr. Masataka Nishikawa and Dr. Noboru Imai for the use of the simulated Asian mineral dust sample (CJ-2) and GSJ reference samples "Igneous rock series", respectively.

References

- 1 D. Zhang, *Scientia Sinica*, **27B**, 825 (1984).
- 2 A. Mizohata and T. Mamuro, *J. Jpn. Soc. Air Pollut.*, **13**, 289 (1978).
- 3 S. Kadowaki, *Environ. Sci. Technol.*, **13**, 1130 (1979).
- 4 Y. Ishizaka and A. Ono, *Idojaras*, **86**, 249 (1982).
- 5 Y. Iwasaka, H. Minoura, and K. Nagaya, *Tellus*, **35B**, 189 (1983).
- 6 Y. Sekine and Y. Hashimoto, *J. Jpn. Soc. Air Pollut.*, **26**, 216 (1991).
- 7 M. Darzi and J. W. Winchester, *J. Geophys. Res.*, **87**, 1251 (1982).
- 8 R. A. Duce, C. K. Unni, B. J. Ray, J. M. Prospero, L. Chen, and J. T. Merrill, *Science*, **209**, 1522 (1980).
- 9 K. Isono, M. Komabayashi, T. Takeda, T. Tanaka, K. Iwai, and M. Fujiwara, *Tellus*, **23**, 40 (1971).
- 10 G. E. Shaw, *J. Appl. Met.*, **19**, 1254 (1980).
- 11 M. Uematsu, R. A. Duce, J. M. Prospero, L. Chen, J. T. Merrill, and R. L. McDonald, *J. Geophys. Res.*, **88**, 5343 (1983).
- 12 K. Okada, H. Naruse, T. Tanaka, O. Nemoto, Y. Iwasaka, P.-M. Wu, A. Ono, R. A. Duce, M. Uematsu, J. T. Merrill, and K. Arao, *Atmos. Environ.*, **24A**, 1369 (1990).
- 13 S. Tanaka, M. Tajima, and Y. Hashimoto, *J. Chem. Soc. Jpn.*, **1986**, 713.
- 14 M. Nishikawa, S. Kanamori, N. Kanamori, and T. Mizoguchi, *J. Aerosol Res. Jpn.*, **6**, 157 (1991).
- 15 M. Nishikawa, S. Kanamori, N. Kanamori, and T. Mizoguchi, *Sci. Total Environ.*, **107**, 13 (1991).
- 16 I. Mori, Y. Iwasaka, M. Nishikawa, and H. Quan, *J. Environ. Chem.*, **6**, 567 (1996).
- 17 T. Kyotani and M. Iwatsuki, *J. Jpn. Soc. Atmos. Environ.*, **35**, 287 (2000).
- 18 A. Mizohata, Y. Matsuda, K. Sakamoto, and S. Kadowaki, *J. Jpn. Soc. Air Pollut.*, **21**, 83 (1986).
- 19 X.-B. Fan, K. Okada, N. Niimura, K. Kai, K. Arao, G.-Y. Shi, Y. Qin, and Y. Mitsuta, *Atmos. Environ.*, **30**, 347 (1996).
- 20 N. Imai, S. Terashima, S. Itoh, and A. Ando, *Geochem. J.*, **29**, 91 (1995).
- 21 E. Thomas and P. R. Buseck, *Atmos. Environ.*, **17**, 2299 (1983).
- 22 J. E. Post and P. R. Buseck, *Environ. Sci. Technol.*, **18**, 35 (1984).
- 23 J. Osán, Sz. Török, K. Török, L. Németh and J. L. Lábár, *X-ray Spectrom.*, **25**, 167 (1996).
- 24 W. Jambers and R. Van Grieken, *Environ. Sci. Technol.*, **31**, 1525 (1997).
- 25 J. Osán, I. Szalóki, C.-U. Ro and R. Van Grieken, *Mikrochim. Acta*, **132**, 349 (2000).
- 26 N. Kaufherr and D. Lichtman, *Environ. Sci. Technol.*, **18**, 544 (1984).
- 27 H. Quan, Y. Huang, M. Nishikawa, X. Liu, I. Mori, Y. Iwasaka, Q. Wei and S. Qiao, *J. Environ. Chem.*, **6**, 225 (1996).
- 28 G.-L. Liu, M. Owari, Y. Sako, H. Egawa, S. Suzuki and Y. Nihei, *Bunseki Kagaku*, **38**, 515 (1989).
- 29 Y. Iwasaka, M. Yamato, R. Imasu and A. Ono, *Tellus*, **40B**, 494 (1988).
- 30 T. Kyotani, M. Iwatsuki and S. Koshimizu, Proc. the 59th Symposium on Anal. Chem., Otaru, 1D17, May (1998).